International Journal of u- and e- Service, Science and Technology
Vol.8, No. 6 (2015), pp.147-160
http://dx.doi.org/10.14257/ijunesst.2015.8.6.14

Research on the Method for Extracting the Cellular Microscopic Digital Features of Coniferous Wood

Lei Zhao[1,a] and Jian Hua Wang[2,b]

[1]*Heilongjiang International University, Harbin, China*
[2]*Harbin normal University, Harbin, China*
[a]*154372732@qq.com*,[b]*wjh@vip.163.com*

Abstract

The cell slices of 5 species of common coniferous wood, including Cupressaceae, Abies nephrolepis, Picea jezoensis var. microsperma, Pinus koraiensis and Pinus massoniana and so on, are analyzed for the establishment of a hexagonal shape to simulate the wood cell structure. By using the image processing technology, the relevant parameters are extracted, including quasi-circular degree, the surface area, perimeter, width and thickness of cells, wall thickness, ratio of wall to cavity, ratio of cavity to diameter and cell density. In the experiment, mathematical analysis was made on 5,000 cells of the 5 species, and the cell sampling section was determined. After sampling, with the parameter values of cells obtained compared to the standard values, the error is within 10%. Afterwards, the value range of the cell parameters of each species is determined, which provides data basis for the recognition of wood species. Experiments show that the algorithm performs with better robustness in the recognition of wood species.

Keywords: *hexagonal shape, quasi-circular degree, cell density, cell slices*

1. Introduction

There are many defects in the application of traditional wood species recognition methods [1-4]. Therefore, it has become an urgent problem, waiting to be solved, to use computer in the identification of wood species. The recognition of wood species in the micro field of cells can effectively solve the bottleneck problem caused by the recognition based on artificial experience [5-6]. The main procedures are: analyze and calculate the annual ring age of the annual ring images photos; select the cells in the annual rings of trees over ten years old and make cell slices; capture the images of the annual rings, veins and cells; make mathematical analysis of the cells in the micro field and abstract the microscopic cellular feature parameters, to identify the wood species [7-10]. However, different image processing methods and different cell parameters will affect the recognition results, so in this paper, some reference values for the identification of wood species are presented, which are based on the parameters including quasi-circular degree, the surface area, perimeter, width and thickness of cells, wall thickness, ratio of wall to cavity, ratio of cavity to diameter and cell density, and the parameter range of common wood species are given. These provide data support for the recognition of wood species.

2. The Definition of Microscopic Cellular Feature Parameter

On the basis of the enlarged images of wood slices and the cell image, as shown in Figure 1 and Figure 2, in order to facilitate the acquisition of experimental data, we establish the mathematical model of the approximately hexagonal structure of board base cells. The parameter definitions of the simulated cell contour and the real cell contour are compared, as shown in Figure 3 (b).

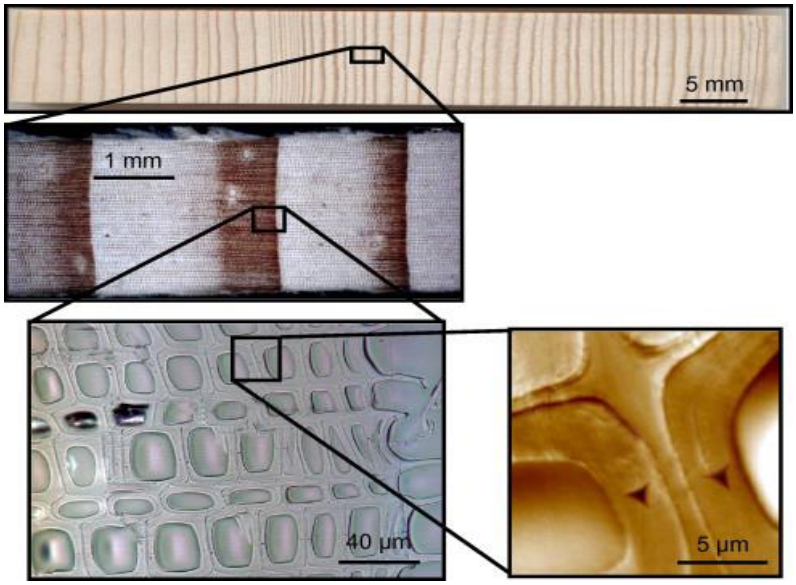

Figure 1. Ring and Cell Larger Image

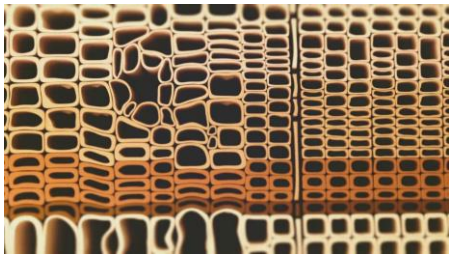

Figure 2. The Cross Section Image of Softwood

(1) Quasi-circular degree

The quasi-circular degree in a broad sense refers to the degree of approximation between an image and a standard circle or oval. In practice, the quasi-circular degree plays an important role.

$$F_1 = \frac{|P_1|}{\sum_{n=1}^{+\infty}(|P_n|+|P_{-n}|)} \tag{1}$$

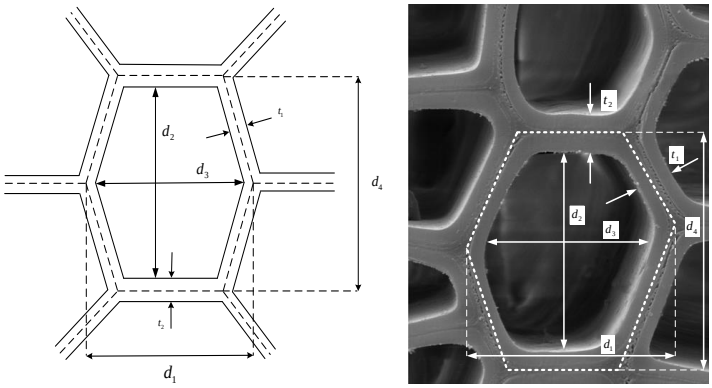

（a）the simulation cell contour **（b）the real cell contour**

Figure 3. Six Prismatic Approximately Simulating Wood Cell Structure Chart

In the chart d_1 refers to chordwise diameter (width), d_2 refers to cell cavity thickness, d_3 cell cavity diameter (chordwise cell cavity), d_4 refers to cell radial diameter (thickness), t_1 tangential wall thickness, t_2 anticlinal wall thickness

In formula1-1, P_n indicates the boundary Fourier coefficient through the chain code method, and the chain codes are c_1, c_2, c_3, … c_i, …, c_M, respectively, which are completed clockwise to the contour curve of cells.

$$P_n \cong \frac{1}{2\pi nj}\sum_{m=1}^{M} a_m e^{j}\left[\frac{\pi}{4}C_m - 2n\pi\frac{\sum_{k=1}^{m} a^k}{\sum_{k=1}^{M} a^k}\right] \tag{2}$$

In this formula, N = ± 1, ± 2, ... ; $a_k = \begin{cases} 1, & if C_k is even; \\ \sqrt{2}, & if C_k is odd; \end{cases}$ k=1, 2, ..., M.

Move the coordinate origin to the centroid, and the parametric equation of the curve C can be written as:

$$U(t) = \sum_{n=1}^{\infty}(P_n e^{jnt} + P_{-n} e^{-jnt}), \quad 0 \le t < 2\pi \tag{3}$$

If the values of all the terms except for $|P_1|$ in the Fourier coefficient P_n are 0, the contour shape indicated by $U(t) = P_1 e^{jt}$ is a circle with a radius of P_1. Then, when C is a circle, its quasi-circular degree will be 1, and when C is other shapes $0 < F_1 < 1$, the features such as translation, rotation, size and starting point will meet invariance [34].

(2) The area and perimeter of cells

There are two common methods for calculating the area:

① Pixel counting method

In the technology of digital image processing, the measurement of the area of a target objective includes the measurement of its interior and boundary points [11-15]. In binary images, the enclosed area is composed of sets of interconnected black pixels in a great number, so the calculation of the number of black pixels in this enclosed area is to solve the area of the object region. Here, the number of pixels is adopted as the unit. Thus, based on this idea, the formula for calculating the area of the object region is:

$$S = \sum_{x=1}^{N}\sum_{y=1}^{M} f(x, y) \tag{4}$$

In this formula, S is the cell area, $f(x, y)$ is the gray value of the pixel of which the abscissa is x and ordinate is y. If the object and its background are represented by 0 and 255, respectively, the calculation of cell area will be the count of $f(x, y) = 0$. In using the pixel counting method to calculate the area, the segment representation the most commonly used.

All the coordinates of the pixels obtained with the chain code method can be connected to the pixels with the same ordinates with lines, and the length of all the segments is the area of the cell, as shown in Figure 5-7. From this, what can be obtained is shown in formula 5:

$$S = \sum_{k=1}^{m} x_{k2} - x_{k1} \tag{5}$$

In formula (5), S indicates the total area of the cell, the endpoint abscissa of each end of the connecting segment with the same vertical within the cell area is x_{k1}, x_{k2}, respectively. m is the total number of segments dividing the cell region.

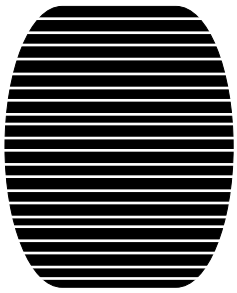

Figure 4. Line Segment Table Notation

② The area calculated by using boundary coordinates

According to Green's Theorem, it can be seen that in a rectangular coordinate system, the area of a closed object area contour can be represented by the integral of the contour curve, which is

$$S = \frac{1}{2}\oint(xdy - ydx) \tag{6}$$

In this formula, the integral is calculated for the target closed contour curve boundary. In practical calculation, to calculate the area covered by the closed contour curve region using Green's theorem, discretization should be carried out first, as shown in formula 7.

$$\begin{aligned} S &= \frac{1}{2}\sum_{i=1}^{N_b}[x_i(y_{i+1} - y_i) - y_i(x_{i+1} - x_i)] \\ &= \frac{1}{2}\sum_{i=1}^{N_b}[x_i y_{i+1} - x_{i+1} y_i] \end{aligned} \tag{7}$$

In this formula, N_b is the number of boundary points, x_i and y_i are the coordinates of the endpoints of the line.

All the aforesaid methods can be used to calculate and measure the area of the target objects, but at the same time, there are many defects. Among them, when using the segment representation method to measure the area, we have to take a variety of complicated boundary conditions into account. The boundary coordinates method does not require the complicated boundary conditions to be considered, but it needs large amounts of calculation and wastes a lot of time. There are a large number of cells contained in the microscopic images of the wood cell slices in this project. If it takes too much time to calculate the area of each cell, the operating efficiency of the system will be greatly reduced. As a result, on the premise of ensuring the accuracy of area calculation, it is also rather crucial to improve the speed of processing.

The accurate detection of the edge of a cell will ensure the accurate morphological analysis of the cell. In the fourth chapter of this paper, the cell contour extraction method based on the edge and regional information has been described, so here it will not be elaborated again. Figure 5 shows the microscopic images of wood cell slices, and the cell area obtained with the method presented in this paper is shown in Table 1.

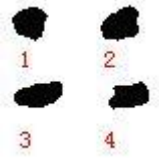

Figure 5. Wood Cell Microscopy Image

Table 1. Area Calculation Results Comparison

Serial number	Area/pixel acquired in other ways	Area/pixel acquired by this project
1	587	589
2	574	574
3	612	613
4	567	568

The contour curve of the target cells obtained with this method is only one pixel wide, so the calculated results are more accurate, compared with the actual cell contour. Moreover, the binary cell images have completely closed cell contour curves, so they can be used to calculate the area and perimeter of cells more accurately.

③ Cell width and thickness

According to the description in Chapter 2, the chain code method makes it easy to use the direction code values to represent the contour point coordinate values. From the hexagonal modeling of cells, we can see that the average width of cells (average tangential diameters) d_1 can be obtained by using formula (8):

$$d_1 = \sum_{i=1}^{n}\left(\max\left\{x_{i_1}, x_{i_2}, x_{i_3}, ..., x_{i_m}\right\} - \min\left\{x_{i_1}, x_{i_2}, x_{i_3}, ..., x_{i_m}\right\}\right) \Big/ n \tag{8}$$

In the formula, $\max\left\{x_{i_1}, x_{i_2}, x_{i_3}, ..., x_{i_m}\right\}$ is the maximum value of the abscissa of the contour point m of cell i, and $\min\left\{x_{i_1}, x_{i_2}, x_{i_3}, ..., x_{i_m}\right\}$ is the maximum value of the abscissa of the contour point m of cell i.

The average thickness of cells (average radial diameters) d_4 can be obtained with formula (9):

$$d_4 = \sum_{i=1}^{n}\left(\max\left\{y_{i_1}, y_{i_2}, y_{i_3}, ..., y_{i_m}\right\} - \min\left\{y_{i_1}, y_{i_2}, y_{i_3}, ..., y_{i_m}\right\}\right) \Big/ n \tag{9}$$

In the formula, $\max\left\{y_{i_1}, y_{i_2}, y_{i_3}, ..., y_{i_m}\right\}$ is the maximum value of the ordinate of the contour point m of cell i, and $\min\left\{y_{i_1}, y_{i_2}, y_{i_3}, ..., y_{i_m}\right\}$ is the maximum value of the ordinate of the contour point m of cell i.

④ Wall thickness

The wall thickness includes the average radial wall thickness and tangential wall thickness. According to the cell model in Figure 5-6, the following formula is obtained:

$$t_1 = \left(d_1 - \left(\sum_{i=1}^{n}\left(\max\left\{x_{i_1}^{'}, x_{i_2}^{'}, x_{i_3}^{'}, ..., x_{i_m}^{'}\right\} - \min\left\{x_{i_1}^{'}, x_{i_2}^{'}, x_{i_3}^{'}, ..., x_{i_m}^{'}\right\}\right)\right) \Big/ n\right) \Big/ 2 \tag{10}$$

In the formula, the average width of the cell d_1 (the average tangential diameter) is

the maximum value of the abscissa of the inner cavity contour point m of cell i, and $\min\left\{x_{i_1}^{'}, x_{i_2}^{'}, x_{i_3}^{'}, ..., x_{i_m}^{'}\right\}$ is the minimum value of the abscissa of the inner cavity contour point m of cell i.

$$t_2 = \left(d_4 - \left(\sum_{i=1}^{n} \left(\max\left\{y_{i_1}^{'}, y_{i_2}^{'}, y_{i_3}^{'}, ..., y_{i_m}^{'}\right\} - \min\left\{y_{i_1}^{'}, y_{i_2}^{'}, y_{i_3}^{'}, ..., y_{i_m}^{'}\right\}\right)\right) \Big/ n \right) \Big/ 2 \quad (11)$$

In this formula, d_4 is the average thickness of the cell (average radial diameter), $\max\left\{y_{i_1}^{'}, y_{i_2}^{'}, y_{i_3}^{'}, ..., y_{i_m}^{'}\right\}$ is the maximum value of the ordinate of the inner cavity contour point m of cell i, and $\min\left\{y_{i_1}^{'}, y_{i_2}^{'}, y_{i_3}^{'}, ..., y_{i_m}^{'}\right\}$ is the minimum value of the ordinate of the inner cavity contour point m of cell i.

⑤ Ratio of wall to cavity and ratio of cavity to diameter

The ratio of wall to cavity refers to the ratio between the radial wall thickness of duple tracheid and the diameter of tangential cell cavity. The cell wall of autumn wood is thick, while that of the spring wood is thin. However, sometimes the absolute thickness of the cell wall of spring wood with a long diameter may not be smaller than that of the autumn wood. The ratio of wall to cavity k_1 is shown by formula (12).

$$k_1 = \frac{2 \times t_2}{d_3} \quad (12)$$

In the formula, t_2 represents the radial wall thickness, t_1 represents the tangential wall thickness and d_3 indicates the cell cavity diameter (tangential cell cavity).

The ratio of cavity to diameter is the ratio between the diameter of the cavity and that of the cell. It shows the degree of fiber flexibility, also known as the flexibility coefficient. The ratio of cavity to diameter k_2 is shown in formula (13).

$$k_2 = \frac{d_3}{d_1} \quad (13)$$

In this formula, d_1 indicates the tangential diameter (width) of the cell, and d_3 represents the diameter of the cell cavity (tangential cell cavity).

⑥ Cell density

Cell density refers to the number of cells per unit of area, used to represent the crowded or loose distribution of wood cells. Cell density ∂ is shown in formula (14) .

$$\partial = \frac{n}{s} \quad (14)$$

In this formula, n indicates the number of cells in the target region of wood slices, and s represents the area of the region.

3. The Calculation and Analysis of the Microscopic Cellular Feature Parameters

Through the mathematical analysis of more than 5,000 cell images of 5 wood species, the standard threshold range of 5 parameters of the board cell is obtained. According to the results, it can be obtained how the width and thickness values of the spring wood and autumn wood of the 5 wood species are distributed, and on the basis of the value distribution, the average width and thickness of cells can be calculated. On drawing, the calculated data is grouped in the unit of 5 microns to determine the sampling interval, and

MATLAB is used for drawing. The results are shown in Figure 6.

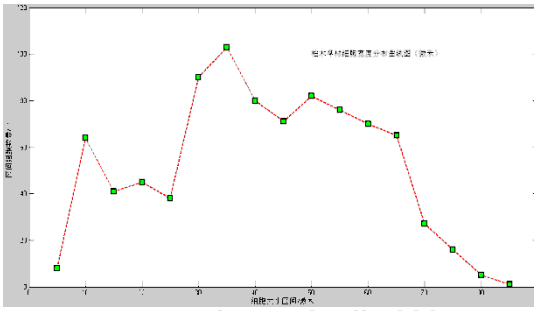

Cypress early wood cell width distribution picture $10 \leqslant \sigma \leqslant 60$

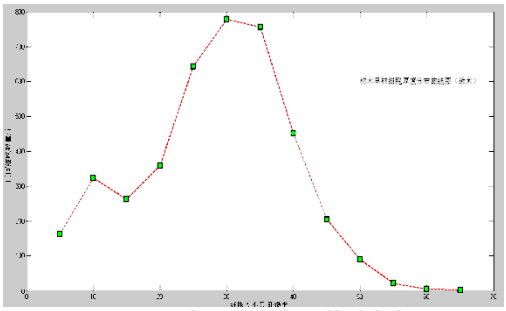

Cypress early wood cell thickness distribution picture $20 \leqslant \sigma \leqslant 40$

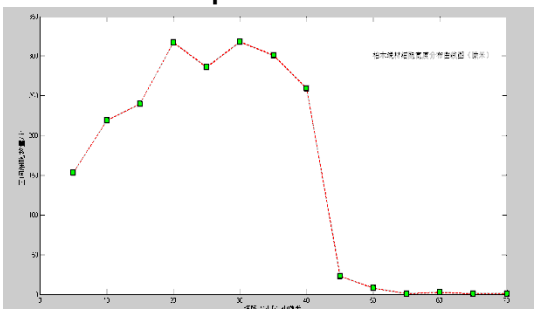

Cypress late wood cell width distribution picture $10 \leqslant \sigma \leqslant 60$

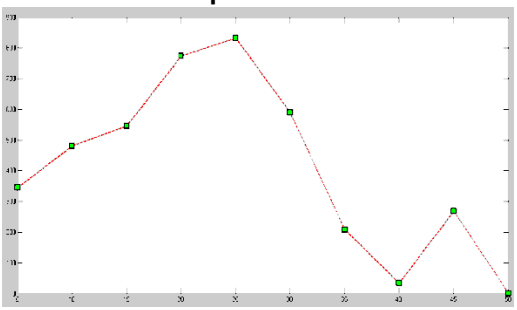

Cypress late wood cell thickness distribution picture $10 \leqslant \sigma \leqslant 60$

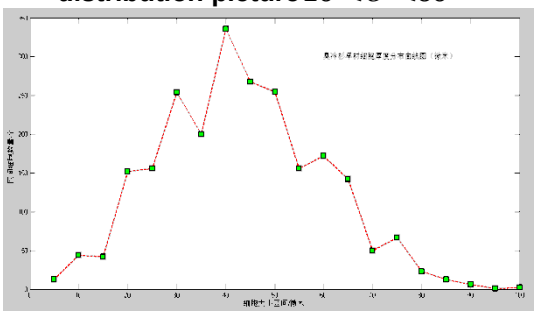

Abies nephrolepis early wood cell width distribution picture $10 \leqslant \sigma \leqslant 60$

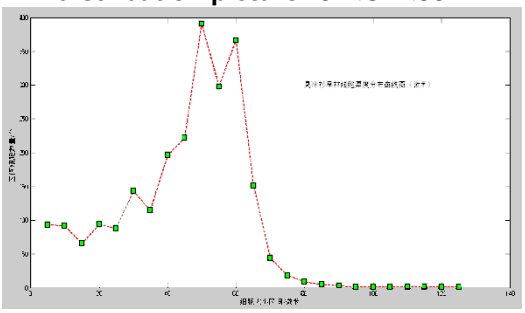

Abies nephrolepis early wood cell thickness distribution picture $10 \leqslant \sigma \leqslant 60$

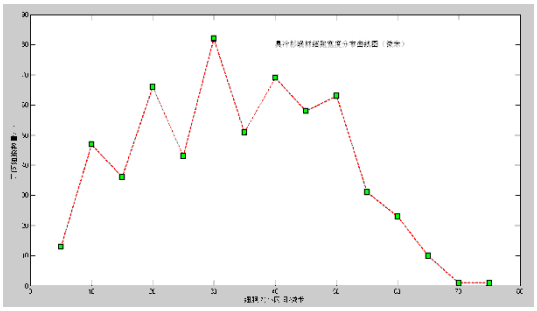

Abies nephrolepis late wood cell width distribution picture $10 \leqslant \sigma \leqslant 60$

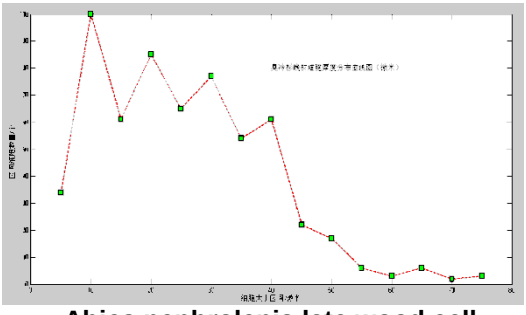

Abies nephrolepis late wood cell thickness distribution picture $10 \leqslant \sigma \leqslant 60$

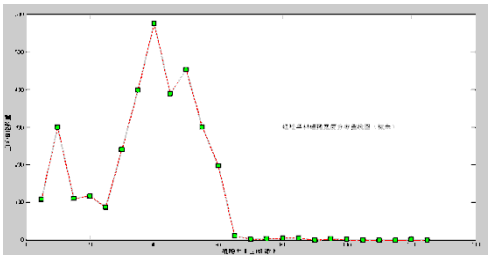

Korean pine early wood cell width distribution picture（$10 \leqslant \sigma \leqslant 60$）

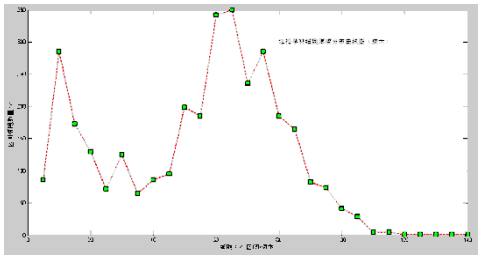

Korean pine early wood cell thickness distribution picture（$10 \leqslant \sigma \leqslant 60$）

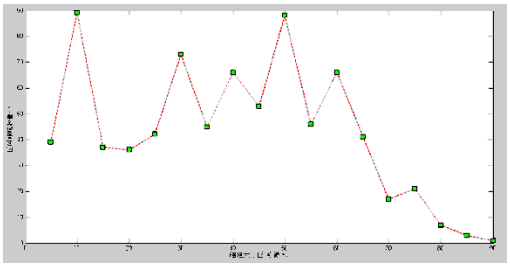

Korean pine late wood cell width distribution picture（$10 \leqslant \sigma \leqslant 60$）

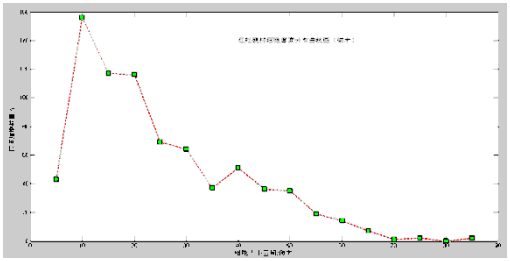

Korean pine late wood cell thickness distribution picture（$10 \leqslant \sigma \leqslant 60$）

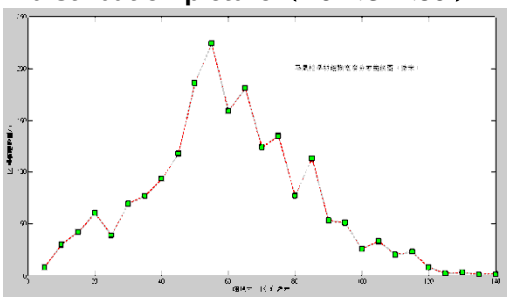

Masson pine early wood cell width distribution picture（$10 \leqslant \sigma \leqslant 60$）

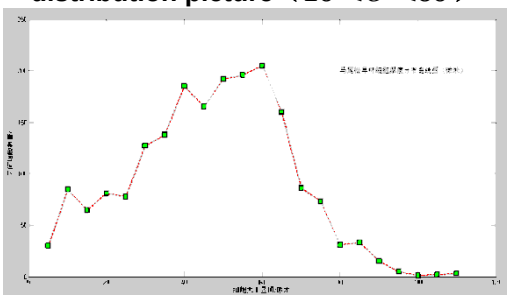

Masson pine early wood cell thickness distribution picture $10 \leqslant \sigma \leqslant 60$

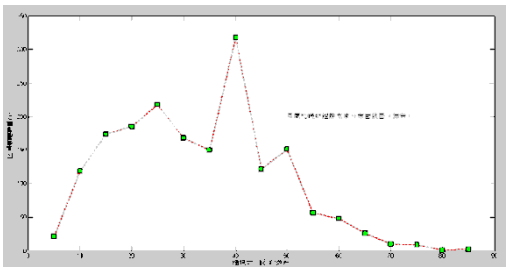

Masson pine late wood cell width distribution picture（$10 \leqslant \sigma \leqslant 60$）

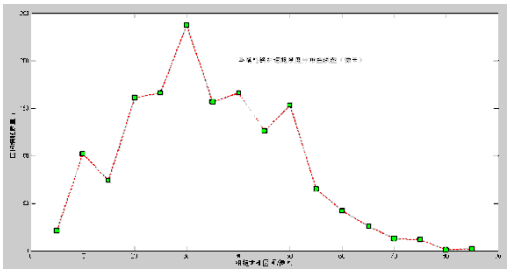

Masson pine late wood cell thickness distribution picture（$10 \leqslant \sigma \leqslant 60$）

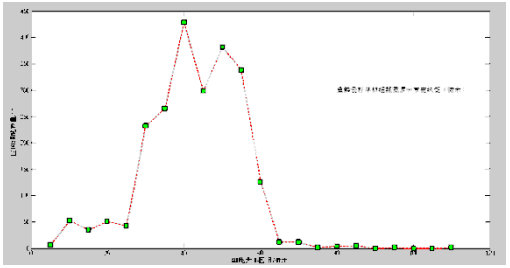

Picea jezoensis early wood cell width distribution picture（$25 \leqslant \sigma \leqslant 50$）

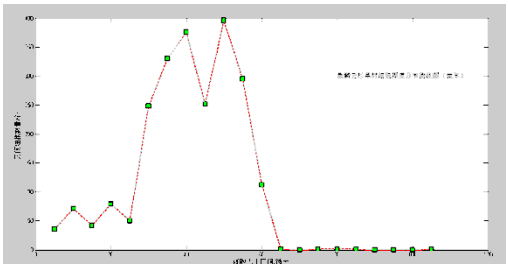

Picea jezoensis early wood cell thickness distribution picture（$25 \leqslant \sigma \leqslant 65$）

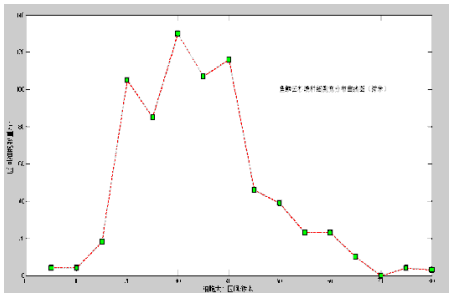

Picea jezoensis late wood cell width distribution picture（20≤σ≤45）

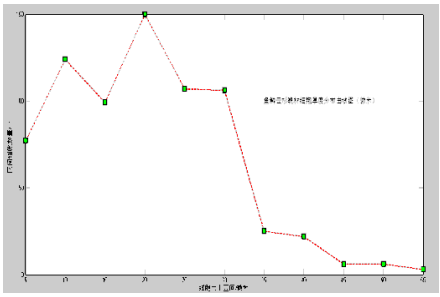

Picea jezoensis late wood cell thickness distribution picture（5≤σ≤30）

Figure 6. The Interval Distribution of Five Kinds of Wood Species of Early and Late Wood Cell Width and Thickness

After sampling the cellular width and thickness of the spring wood and autumn wood of the 5 species, with the description of the tracheid morphology table of the 5 species in Wood Identification - Major Tree Species as reference data, it is found through experimental comparison that the range of the error between calculated values and values in the reference book is within 10%, as shown in Table 2.

Table 2. The Comparison Table of The Calculation Results Of This Subject's Width And Thickness With The Standard Values

	Standard values						The calculation results of this subject					
	Width (micron)（average chord wise diameter）			Thickness (macron)（average radial diameter）			Width (macron)（average chord wise diameter）			Thickness (macron)（average radial diameter）		
	early wood	late wood	late/early	early wood	late wood	late/early	early wood	late wood	late/early	early wood	late wood	late/early
Cypress	33	30	0.91	38	24	0.63	35.40	29.07	0.82	38.72	25.34	0.65
Abies nephrolepis	32	31	0.97	48	24	0.50	35.19	31.45	0.89	50.34	23.05	0.46
Picea jezoensis	36	32	0.89	41	19	0.46	39.61	30.44	0.75	40.77	17.80	0.39
Korean pine	42	39	0.93	57	23	0.40	42.06	35.01	0.83	57.65	21.15	0.35
Masson pine	45	42	0.93	58	29	0.50	40.48	40.98	1.01	57.20	31.72	0.55

According to Table 2, a table of the range of errors between width and thickness can be obtained, as shown in Table 3.

Table 3. Width and Thickness Deviation Statement

	Width (macron)deviation（average chord wise diameter）		Thickness (macron)deviation（average radial diameter）	
	early wood	late wood	early wood	late wood
Cypress	7.273%	3.100%	1.895%	5.583%
Abies nephrolepis	9.969%	1.452%	4.875%	3.958%
Picea jezoensis	10.028%	4.875%	0.561%	6.316%
Korean pine	0.143%	10.231%	1.140%	8.043%

Masson pine	10.044%	2.429%	1.379%	9.379%

It can be seen by analyzing the data in Table 2 that the tracheid width of the spring wood of the 5 species is within the range of 35.19 μm ~ 42.06 μm, and that of the autumn wood is within the range of 29.07 μm ~40.98 μm. The total average width of spring wood and autumn wood is 38.548 μm and 33.39 μm, respectively, with a gap of 13% between them. This means that the width of the spring wood and autumn wood is basically the same. Because they show a positive radial array relationship, there tends to be a smaller gap between tracheid widths. The maximum value of the tracheid width of the spring wood is that of Pinus koraiensis, which is 42.06 μm, and the minimum value is that of Abies nephrolepis, which is 35.19 μm. The gap between the maximum and minimum values is 16.3%. The maximum value of the tracheid width of the autumn wood is that of Pinus massoniana, which is 40.98 μm, while the minimum value is that of Cupressaceae, which is 29.07 μm. The gap between the maximum and minimum values is 29.06%.

The tracheid thickness of the spring wood of the 5 species is in the range of 38.72 μm ~58.65 μm, and that of the autumn wood is in the range of 17.80 μm ~31.72 μm. The total average thickness values of spring wood and autumn wood are 48.936 μm and 23.812 μm, respectively, with a gap of 51.34%. This means that the tracheid of the spring wood is thicker than that of autumn wood. Furthermore, by observing the microscopic images, it can be seen obviously that there is a much larger gap between the spring wood at the beginning point of growth ring and the autumn wood at the end of growth ring. The maximum value of the tracheid width of the spring wood is that of Pinus koraiensis, which is 57.65 μm, and the minimum value is that of Cupressaceae, which is 38.72 μm. The gap between the maximum and minimum values is 32.84%. The maximum tracheid width of the autumn wood is that of Pinus massoniana, which is 31.72 μm, and the minimum value is that of Picea jezoensis var. microsperma, which is 17.80 μm. The gap between the maximum and minimum values is 43.89%.

Table 4. Tangential Wall/Anticlinal Wall Thickness Computing Results

	Standard values						The calculation results of this subject					
	tangential wall thickness(macron)			anticlinal wall thickness (macron)			tangential wall thickness(macron)			anticlinal wall thickness (macron)		
	early wood	late wood	late/early	early wood	late wood	late/early	early wood	late wood	late/early	early wood	late wood	late/early
Cypress	4.0	4.5	1.26	3.7	4.6	1.24	3.82	4.73	1.23	3.93	4.54	1.56
Abies nephrolepis	2.9	4.4	1.52	2.7	4.2	1.56	2.61	4.12	1.59	2.34	4.63	1.98
Picea jezoensis	2.3	3.7	1.61	2.3	4.3	1.87	2.53	3.36	1.33	2.06	4.69	2.28
Korean pine	3.1	4.4	1.42	2.9	5.5	1.90	3.55	4.84	1.36	3.35	5.26	1.57
Masson pine	3.0	6.2	2.07	2.5	5.9	2.36	2.64	5.71	2.16	2.73	6.52	2.39

According to Table 4, a table of the range of errors between wall thicknesses can be obtained, as shown in Table 5.

Table 5. Tangential Wall/Anticlinal Wall Thickness Deviation Statement

	Average tangential wall thickness (macron) deviation（average chordwise diameter）s		Average anticlinal wall thickness (macron) deviation （average radial diameter）	
	early wood	late wood	early wood	late wood
Cypress	4.50%	5.11%	6.22%	1.30%
Abies nephrolepis	10.00%	6.36%	13.33%	10.24%
Picea jezoensis	10.00%	9.19%	10.43%	9.07%
Korean pine	14.52%	10.00%	15.52%	4.36%
Masson pine	12.00%	7.90%	9.20%	10.51%

It can be seen by analyzing the data in Table 4 that the average tracheid tangential wall thickness of spring wood of the 5 species is 3.03 μm, and that of the autumn wood is 4.55 μm, with a gap of 33.41% between them. This means that the tangential wall of spring wood is much thinner than that of autumn wood. Through comprehensive analysis of the spring and autumn wood, the tangential wall thickness of Cupressaceae is relatively thicker, while that of Picea jezoensis var. microsperma is relatively thinner. The tracheid radial wall thickness of autumn wood is greater than that of spring wood. The total average tracheid radial wall thickness of spring wood and autumn wood is 2.882 μm and 5.128 μm, respectively. There is a gap of 43.8% between them. Among the spring wood, the radial wall of Cupressaceae is the thickest, while among the autumn wood, the radial wall of Pinus massoniana is the thickest. By analyzing the radial and tangential wall thickness of spring and autumn wood of the 5 wood species, it can be seen that the radial and tangential wall thickness of spring wood are basically the same, with a gap of only 4.88% between the average values. The radial wall of autumn wood is 11.2% thicker than that of spring wood. Moreover, the calculated data is basically consistent with the definition of autumn wood: the tracheid in which the shared tangential wall between duplex cells is greater than or equal to the radial diameter of the cell cavity is autumn wood.

Table 6. Wall Cavity Ratio /Cavity Diameter Ratio Calculation Results

	Standard values				The calculation results of this subject			
	Wall cavity ratio		cavity diameter ratio		Wall cavity ratio		cavity diameter ratio	
	early wood	late wood	early wood	late wood	early wood	late wood	early wood	late wood
Cypress	0.29	0.44	0.78	0.69	0.285	0.454	0.822	0.688
Abies nephrolepis	0.20	0.37	0.83	0.73	0.153	0.417	0.867	0.706
Picea jezoensis	0.15	0.37	0.87	0.73	0.116	0.445	0.896	0.692
Korean pine	0.16	0.39	0.86	0.72	0.189	0.429	0.841	0.699
Masson pine	0.13	0.39	0.89	0.72	0.156	0.467	0.865	0.682

According to Table 6, an error range table of wall-cavity ratio and cavity-diameter ratio can be obtained, as shown in Table 7.

Table 7. Wall Cavity Ratio /Cavity Diameter Ratio Deviation Statement

	Wall cavity ratio		cavity diameter ratio	
	early wood	late wood	early wood	late wood
Cypress	1.72%	3.18%	5.38%	0.29%
Abies	23.50%	12.70%	4.46%	3.29%

nephrolepis				
Picea jezoensis	22.67%	20.27%	2.99%	5.21%
Korean pine	18.13%	10.00%	2.21%	2.92%
Masson pine	20.00%	19.74%	2.81%	5.28%

Because in the technology of digital image processing, a pixel is used as the basic unit for image processing, to make more accurate analysis of actual cells, we must convert pixel values into micron. In terms of the international system of units: 1 inch = 25400 microns [77-78], we can get the following method for unit conversion:

$$X_{\mu m} = \frac{25400 * X_p}{P_{in} * N} \tag{15}$$

In the formula (15), $X_{\mu m}$ and X_p are the value of sliced cells and the displayed value of microscopic sliced images, respectively. P_{in} is the number of pixels on an inch of the monitor screen, and N is the enlarged times of cell images.

Table 8. 5 Kinds of Trees Early Wood Parameter Range

early wood	Cell area region	area average after shampling	Cell perimeter region	Perimeter average after shampling	Tangential diameter region	Tangential diameter averager after shampling	Radical diameter region	Radical diameter average after shampling	Roundness region	mean cell density/mm2
Cypress	15.5~4958.6	765.4	15.52~622.3	121.94	3.41~90.3	35.40	4.23~63.5	38.72	0.69~2.97	292
Abies nephrolepis	19.75~5589.41	1458.98	16.93~740.83	176.69	1.41~138.28	35.19	1.41~122.766	50.34	0.78~2.99	267
Picea jezoensis	15.52~6454.42	1698.75	15.43~636.41	185.88	2.82~131.23	39.61	1.42~104.42	40.77	0.57~2.81	163
Korean pine	15.61~7202.31	1567.55	15.57~928.51	182.79	1.43~172.34	42.06	1.46~238.47	57.65	0.72~2.84	249
Masson pine	16.93~9398.53	1650.77	16.87~553.15	178.67	1.42~193.32	40.48	1.44~118.53	57.20	0.75~2.93	231

According to the definition of numerical parameters of cells, the calculation results and ranges of relevant parameters are shown in Table 8 and Table 9 (the unit of all parameters are micron, except the quasi-circular degree and average density of cells). From the data in Table 8 and Table 9, it can be seen that the tracheid area of the spring and autumn wood of Picea jezoensis var. microsperma is the largest. The average tracheid area of the spring wood and autumn wood is 1698.75 and 609.90, respectively. The tracheid area of the spring and autumn wood of Cupressaceae is the smallest. The average tracheid area of the spring wood and autumn wood is 765.4 and 422.639, respectively. Therefore, the tracheid density of Picea jezoensis var. microsperma is the smallest, while that of Cupressaceae is the largest.

Table 9. 5 Kinds of Trees Late Wood Parameter Range

Late wood	Cell area region	area average after shampling	Cell perimeter region	Perimeter average after shampling	Tangential diameter region	Tangential diameter averager after shampling	Radical diameter region	Radical diameter average after shampling	Roundness region	mean cell density/ mm2
柏木	11.52~2690.98	422.639	15.52~ 503.76	88.97	1.41~ 217.32	29.07	1.42~ 69.14	25.34	0.69~ 2.97	523
臭冷杉	16.93~2967.56	503.20	15.79~ 430.38	98.70	1.46~ 84.66	31.45	1.41~ 73.27	23.05	0.78~ 2.87	442
鱼鳞云杉	18.34~4230.51	609.90	15.52~ 314.67	110.19	4.23~ 103.02	30.44	1.46~ 90.31	17.80	0.68~ 2.88	289
红松	15.52~3138.31	526.39	15.58~ 400.76	109.89	1.41~ 84.67	35.01	1.41~ 134.05	21.15	0.82~ 2.89	451
马尾松	15.50~4167.01	602.10	15.59~ 304.82	102.76	1.43~ 93.13	40.98	1.43~ 83.25	31.72	0.64~ 2.84	293

4. Conclusion

In this paper, a recognition algorithm based on the cellular microscopic digital features, to extract the relevant parameters of board cell images, including quasi-circular degree, the area, perimeter, width and thickness of cells, wall thickness, ratio of wall to cavity, ratio of cavity to diameter and cell density and so on. The calculated results obtained are compared to the standard values, and through analysis, it is found that the error range is basically within 10%. The digital image processing technique is used to extract the mathematical feature parameters of cells, and the wood species are judged according to the standard parameter database. By using this method, the speed of wood species recognition can be improved, and it can also effectively reduce the instability due to the high dependence of the recognition method on the pixel feature of images. The method has a high recognition accuracy and robustness. Moreover, this method also gets rid of the restriction of wood species recognition on the experience of operators, to study the microscopic field of wood cells, which is of great significance to wood species recognition. However, the wood cells are affected by various factors, such as temperature, humidity and so on, and the samples for experiment are not diversified enough. Therefore, as the follow-up experiment progresses, it will be a work focus to constantly update the experimental database of samples.

References

[1] W. Yuanquan, T. Min, P. A. Heng, X. Deshen and X. Ye, "Research on Boundary Concavities Segmentation via Snake Models", Journal of Computer Research and Development, vol. 42, no. 7, pp. l179- ll84.
[2] C. Can, Z. Guo-Hua and L. Bao-Zhong, "Adaptive Wave-Gate Tracking Algorithm Based on Snake Model", Electronics Optics & Control, vol. 21, no. 1, **(2014)**, pp. 78-85.
[3] Z. Huanhui, "Research on Technology of Medical Image Segmentation Based on GVF Snake Model", Shandong University, Shandong, **(2010)**.
[4] X. N. Wang, Y. J. Feng and Z. R. FENG, "Snakes: ant colony optimization for image segmentation", IEEE, Trans. Guangzhou, The Fourth International Conference on Machine Learning and Cybernetics, vol. 1, **(2005)**, pp. 5355 -5360.
[5] J. B. Fasquel, "An Interactive Medical Image Segmentation System Based on The Optimal Management of Regions of Interest using Topological MedicalKnowledge", Computer Methods and Programs in Biomedicine, vol. 82, no. 3, pp. 216-230.
[6] B. Kai, L. Min and X. Jing, "Fusion of Snake model and topological alignments algorithm for image segementation", Application Research of Computers, vol. 30, no. 2, **(2013)**, pp. 610-612.
[7] MIURAK, "Tracking movement in cell biology", Advances in Biochemical Engineering/Biotechnology, vol. 95, no. 2, **(2004)**, pp. 267-295.
[8] H. Qing and L. Mishnaevsky, "Moisture-related mechanical properties of softwood: 3D micromechanical modeling Hai Qing, Leon Mishnaevsky", Computational Materials Science, vol. 46, **(2009)**, pp. 310~320.
[9] M. Yang, K. Kidiyo and R. Joseph, "A survey of shape feature extraction techniques", Pattern

Recognition, INTECH, no. 169, **(2010)**, pp. 106~115.
[10] J. Krepkowski, "Growth dynamics and potential for cross-dating and multi-century climate reconstruction of Podocarpus falcatus in Ethiopia", dendrochronologia, no. 30, **(2012)**, pp. 257~265.
[11] H. Shuang-Xi, Z. Shao-Jun, X. Jing-Liang and Y. Chun-Yan, "Extracting profile feature points by a method based on arc length", Photoelectric engineering, vol. 31, no. 11, **(2004)**, pp. 59~62.
[12] Z. Jun, L. Zhengwen, M. A. Zhaorui and P. Jiluan, "Extraction of outline feature points based on the minim um approach error", Journal of tsinghua university, vol. 48, no. 2, **(2008)**, pp. 166~168.
[13] X. Feng, "Comparative study of boundary feature description methods for similar Figure", Shu Zou University, **(2006)**.
[14] B. I. Hassel, P. Berard, C. S. Moden and L. A. Berglund, "The single cube apparatus for shear testing – full-field strain data and finite element analysis of wood in transverse shear", Compos Sci Technol., vol. 69, **(2009)**, pp. 77~82.
[15] A. Manceau, M. L. Schlegel, M. Musso, V. A. Sole, C. Gauthier, P. E. Petit and F. Trolard, Geochim Spectrochim Acta, vol. 64, **(2000)**, pp. 36~43.

Author

Zhao Lei, received his BS in Computer science and technology from Northeast Forestry University, Harbin, China, in 2005. He got his MS in Computer application technology from Northeast Forestry University, Harbin, China, in 2009. He got his ph.d in Forestry Engineering Automation from Northeast Forestry University, Harbin, China, in 2013.He is an Associate Professor in the School of Hei LongJiang International University. His research interests include pattern recognition and intelligent control.

